Top Catal (2010) 53:1340–1348
DOI 10.1007/s11244-010-9592-7

ORIGINAL PAPER

The Influence of Si/Al Ratio on the Distribution of OH Groups in Zeolites with MWW Topology

Barbara Gil · Bartosz Marszałek · Anna Micek-Ilnicka · Zbigniew Olejniczak

Published online: 5 October 2010

Abstract A series of MWW-type zeolites of increasing Si/Al ratio were investigated with respect to their acidic properties. Concentration of the Brønsted acid centers located at the external crystal surface was invariant for the entire series. Ethanol conversion to ethyl-*tert*-butyl ether, proceeding only at the external surface, was also constant. The OH groups in MWW zeolites were found to be homogeneous with proton affinity value equal to 1142.7 kJ/mol.

Keywords MWW zeolites · ETBE synthesis · External surface acidity · IR and NMR studies

1 Introduction

The acidity of zeolites has been extensively studied over past decades [1–3]. As a result, more and more detailed knowledge about this complex phenomenon is being acquired, enabling not only better understanding of the properties of existing and functioning catalysts but also invention and tailoring the new ones. Real catalytic studies require not only the knowledge about the concentration of acid sites but also on their relative strength, availability and type and to achieve this goal multiple probe molecules are employed [4, 5]. The acidity of the external surface of zeolites has gathered a lot of attention, mainly in the aspect of enhancing the shape selectivity of zeolites by passivating their external surface activity [6, 7].

The properties of zeolite MCM-22 [8] and its isomorphous structures ITQ-1 [9, 10], SSZ-25 [11], PSH-3 [12], and ERB-1 [13] have been thoroughly investigated for many years. MWW zeolites crystallize in the form of thin platelets with thickness in the range of just few framework layers. The layers contain two non-intersecting pore systems, both accessible through 10-rings only. One is a two-dimensional sinusoidal channel with uniform, 10-ring diameter (4.1 × 5.1 Å) throughout the structure. The other is formed by the series of supercages of diameter equal to 7.1 Å (12-rings) with unusually large inner height of 18.2 Å, accessible through the elliptic 10-ring openings (4.0 × 5.5 Å).

One of the peculiarities of the MCM-22 zeolite is the fact that it can be formed via two different synthesis methods: either by calcination of the layered precursor MCM-22(P) or by a direct hydrothermal synthesis from a reaction gel. This property is slowly emerging as a more general trend for zeolites [14]. Another rarity presented by the MCM-22 is the unusually large ^{29}Si MAS-NMR shift range (ca. 15 ppm), pointing to large distribution of crystallographic environments present in this structure. Although both hexagonal and orthorhombic forms may be proposed for the MCM-22 zeolite [15, 16], the NMR data determined on highly-siliceous zeolites favor the orthorhombic one with 13 non-equivalent T-sites, one of them being 'buried' within the structure, not accessible from either channel systems [17]. The sitting of aluminum, both in the parent samples [18], and modified by dealumination or desilication [19] has also been investigated.

B. Gil (✉) · B. Marszałek
Faculty of Chemistry, Jagiellonian University,
Ingardena 3, 30-060 Kraków, Poland
e-mail: gil@chemia.uj.edu.pl

A. Micek-Ilnicka
Institute of Catalysis and Surface Chemistry,
Niezapominajek 8, 30-239 Kraków, Poland

Z. Olejniczak
Institute of Nuclear Physics, Radzikowskiego 152,
31-342 Kraków, Poland

MCM-22 (and MCM-49), in contrast to majority of other zeolites, contain hydroxyl groups located at the external surface of the zeolite crystals, namely inside the 12-ring pockets ('cups'). Such protons are responsible for the catalytic activity in hydrocarbons transformation, like alkylation of benzene with ethene and propene among others [20–22]. For that reason investigation of the specific location of acidic hydroxyl groups in the framework of the MWW-type zeolite is of vital importance.

According to literature [16, 23], the synthesis method may influence some of the properties of MWW zeolites, for that reason in the current work the MCM-22 zeolites originating from different laboratories as well as MCM-49 zeolite are investigated.

The goal of this work is to present the uniqueness of some of the features for series of the MWW zeolites, i.e. MCM-22 and MCM-49, differing in the Si/Al ratio. Discussion on the distribution of the framework Al atoms and thus acidic hydroxyl groups responsible for the catalytic activity of these zeolites is also presented. The novelty of this work is detailed characterization of the acid properties of the MWW zeolites (MCM-22 and MCM-49) including the quantification of the external acid sites and its comparison to the catalytic activity of the reaction catalyzed exclusively on the external acid sites.

2 Experimental

MCM-22 and MCM-49 samples were kindly provided by J. Čejka and B. Sulikowski (MCM-22/*29* sample). Chemical composition of the zeolite samples was determined by X-ray fluorescence analysis using a spectrometer Philips PW 1404 provided with an analytical program UniQuant.

Solid state Magic-Angle-Spinning Nuclear Magnetic Resonance (MAS-NMR) spectra were acquired on the APOLLO console (Tecmag) at the magnetic field of 7.05 T (Magnex). For the ^{29}Si MAS-NMR spectra a 3 μs rf pulse ($\pi/2$ flipping angle) was used, 4 kHz spinning speed, and 256 scans with the delay of 40 s were acquired. The ^{27}Al spectra were recorded using the 2 μs rf pulse ($\pi/6$ flipping angle), 8 kHz spinning speed, and 1,000 scans with acquisition delay 1 s.

The acidity was investigated by adsorption of CO, pyridine and pivalonitrile used as probe molecules, followed by FTIR spectroscopy. All samples were activated in the form of self-supporting wafers (ca. 5 mg cm^{-2}) at the conditions given below under vacuum prior to adsorption of the probe molecules. The adsorption temperatures were: carbon monoxide at −100 °C, pyridine at 170 °C, and pivalonitrile at RT. Spectra were recorded on a Bruker Tensor 27 spectrometer, equipped with an MCT detector, working at 2 cm^{-1} resolution. All measured spectra were recalculated to a 'normalized' wafer of 10 mg (density 3.2 g cm^{-2}).

Samples are designated as MCM-22/*n*, where *n* is the Si/Al ratio from the IR analysis. Textural properties of the studied samples were already presented elsewhere [24, 25].

Ethyl alcohol (p.p.a., 96%, POCh Gliwice), isobutene (p.a., Aldrich), *tert*-butyl alcohol (Aldrich) and ethyl-*tert*-butyl ether (ETBE) (99%, Aldrich) were used in the catalytic experiments. The test reaction of ETBE was carried out in a quartz constant flow differential microreactor (ϕ = 10 mm). The helium carrier gas was first saturated with ethanol vapor and subsequently mixed with a stream of isobutene. The composition of the reaction mixture (isobutene/ethanol molar ratio) was equal to one. The catalytic reactor was connected on line with the Perkin-Elmer AutoSystem XL gas chromatograph and a Porapak QS column was used for the chromatographic analyses. Before catalytic experiments the ammonium forms of zeolites were activated ex situ at 500 °C to obtain the acidic forms. After that, the 0.1 g samples of selected zeolites were preheated at 200 °C for 30 min in situ in the catalytic reactor (in helium flow of 30 mL/min) to remove adsorbed water. Catalytic experiments were carried at 80 °C. Each measurement was repeated five times to obtain a representative average.

3 Results and Discussion

FTIR spectroscopy is a direct method of acidity measurement and offers only indirect evidence about the location of Al atoms, since not all aluminum atoms form acidic Si–OH–Al groups. On the other hand, only those Al atoms which are in fact connected with acidic hydroxyls are interesting from the catalytic point of view [26, 27].

IR spectra in the region of OH vibrations were recorded at low temperature (ca. −100 °C) to allow for better apparent resolution (Fig. 1a). There are several bands of hydroxyl groups present in all zeolites under study. Three bands are characteristic of different silanol groups—terminal silanols at 3,750 cm^{-1}, hydrogen-bonded silanols at 3,743 cm^{-1} and geminal silanols at 3,733 cm^{-1}. The presence of the band at 3,733 cm^{-1} depends on the activation temperature. Condensation of the 3,733 cm^{-1} silanols leads to formation of isolated silanol groups—decrease of the band at 3,733 cm^{-1} is accompanied by the intensity increase of the band at 3,750 cm^{-1} (Fig. 1b). In most of the studies reported in the literature, MWW-type zeolites are activated at quite high temperatures (usually well above 500 °C) and therefore the band due to geminal silanols is absent in the majority of them. The band at 3,670 cm^{-1} present in MCM-49 alone is characteristic of extraframework Al species containing its own OH groups;

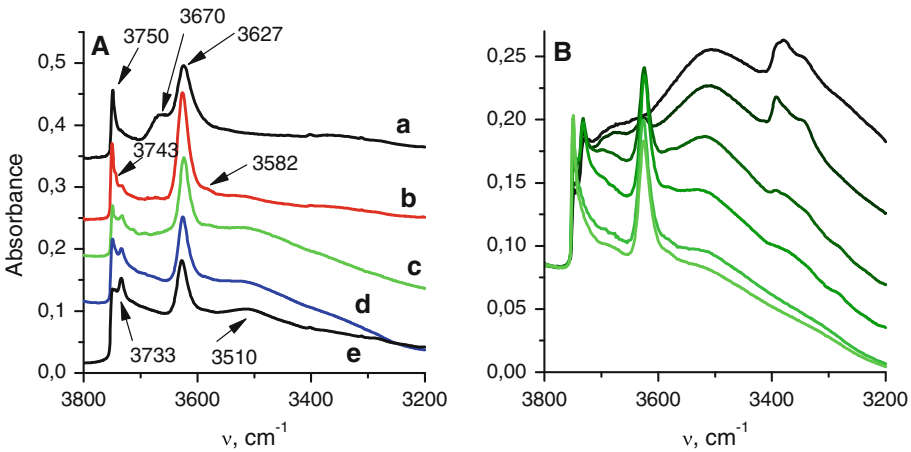

Fig. 1 IR spectra in the region of OH vibration (all spectra normalized to 10 mg pellet). **a** MWW zeolites activated at 500 °C: MCM-49 (*a*), MCM-22/*10* (*b*), MCM-22/*21*(*c*), MCM-22/*29* (*d*) and MCM-22/*40* (*e*). **b** MCM-22/*29* activated at increasing temperatures: from top to bottom 100–700 °C (with 100 °C interval)

this band is absent from other zeolites. Such a band is usually present in high silica zeolites at the lowest region of Si/Al or ultrastabilized zeolites [28]. Usually, the presence of such extraframework Al atoms is not connected with the occurrence of the 0 ppm signal in the ^{27}Al MAS-NMR spectrum [29] because such species cannot form symmetric $[Al(H_2O)_6]^{3+}$ complexes due to the presence of strongly bonded OH group. Moreover, some of these aluminum-containing species reveal the Brønsted-type acidity. In the region of the acidic Si–OH–Al groups two bands can be easily distinguished—at 3,627 cm^{-1} of acidic hydroxyls in 12-ring and 10-ring channels and 3,582 cm^{-1} of OH groups located in hexagonal prisms in between supercages [30]. The amount of OH groups in hexagonal prisms seems to be constant in all MCM-22 zeolites while this band is practically absent in MCM-49, which is the sample with the highest Al content (Si/Al = 12). At the lowest presented region the band at 3,510 cm^{-1} can be observed, assigned to silanol nests. Their presence is indicative of the framework disorder and for this series, as anticipated, is increasing with the increased amount of Al although in none of the cases the intensity of this band is significant.

One of the basic features of zeolites is the ratio between framework Si and Al atoms, which quantitatively characterizes acidity of each sample. To measure the total concentration of acidic species, the experiments of pyridine adsorption was performed. Since MCM-22 (and MCM-49) are very unique zeolites, as the first step the experiments determining the value of the absorption coefficient of pyridinium ions (PyH^+ at 1,545 cm^{-1}) was made. Pyridine was adsorbed in MCM-22/*10* containing only small amount of extraframework Lewis sites, which were saturated during the adsorption of the first pyridine dose. This spectrum was consequently not used for the calculation of the absorption coefficient, according to the procedure described in details in one of our previous publications [31]. The value of the PyH^+ 1,545 cm^{-1} band absorption coefficient determined in that experiment was equal to 0.044 cm/μmol. The absorption coefficient for pyridine bonded to Lewis sites was taken from our earlier work [32]. On the basis of these values and the intensity of the proper IR bands after pyridine adsorption and subsequent evacuation at 250 °C the Si/Al ratio and the number of Lewis sites for all samples were calculated. The high desorption temperature was chosen because of very strong interaction between silanol groups and pyridine. The band of pyridine bonded to SiOH groups at 1,445 cm^{-1} in most cases vanished only after desorption at 250 °C, therefore the intensity of the 1,455 cm^{-1} band of pyridine coordinated to the Lewis sites could be determined with better accuracy. All Si/Al values determined on this basis are close to the ones derived from the XRF analysis of non-calcined samples. This shows that two steps of the thermal treatment—calcination in order to remove template and further activation transforming ammonium form of the zeolite into protonic one (both at 500 °C) are not causing significant dealumination of the samples, which will be further confirmed by the ^{29}Al MAS-NMR. The number of Lewis acid sites for all MCM-22 samples was around 7% and for MCM-49 ca. 10% of all acidic centers present. What is interesting, in the MCM-49 zeolite the part of the band due to extraframework aluminum at 3,670 cm^{-1} is disappearing after pyridine adsorption, as showed in Fig. 2. This means that there are two types of extraframework aluminum species in MCM-49—one displaying Brønsted acidity (band at 3,654 cm^{-1}) and the other, at 3,668 cm^{-1}, non-acidic. The latter band is slightly blue-shifted after pyridine adsorption, which is sometimes observed during pyridine adsorption [33]. For all zeolites the OH groups in hexagonal prisms (band at 3,582 cm^{-1}) are interacting with pyridine because even if pyridine is not able to enter hexagonal prisms, it is able to withdrawn protons from their original positions [5]. During thermodesorption this band is not restored after pyridine desorption at 520 °C (spectra not shown). This

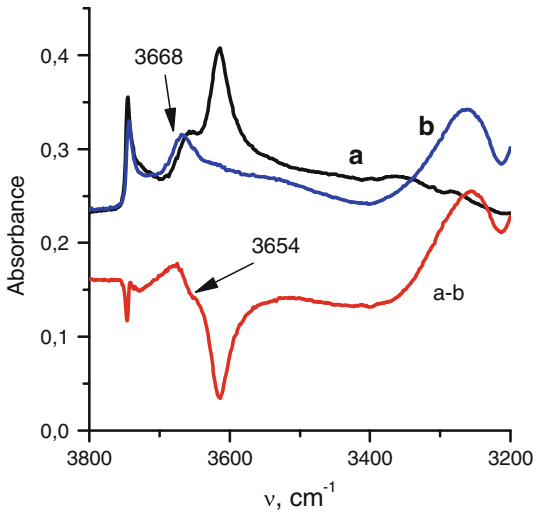

Fig. 2 Spectra of the OH groups in zeolite MCM-49 during pyridine adsorption. *a* spectrum of activated zeolite, *b* after pyridine adsorption and desorption at 250 °C, (*a*−*b*) difference spectrum. All spectra at 170 °C

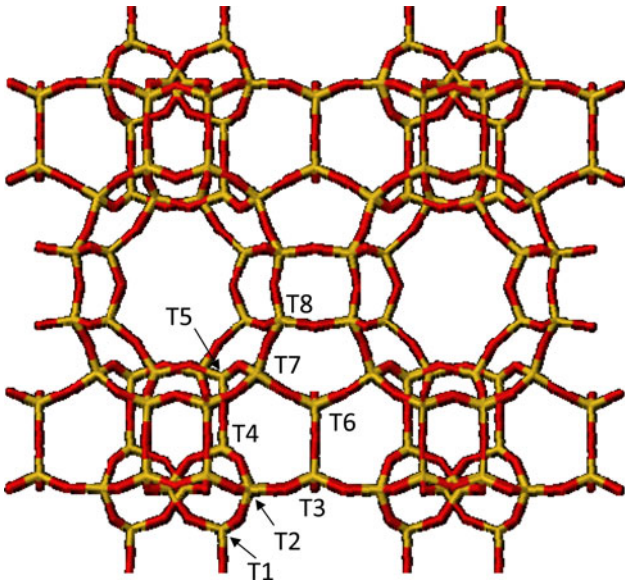

Fig. 3 Schematic illustration of one layer of MCM-22 showing non-equivalent Td positions

could serve as the additional evidence that such OH groups are indeed located in the environment from which the desorption of pyridine is difficult.

For most of the zeolites, the Si/Al ratio determined on the basis of the ^{29}Si MAS-NMR and IR spectroscopy match very well. In the case of MCM-22 zeolites, however, chemical shift of the Si signals depends strongly on the geometric environment of each Si site (Fig. 3). The signal at −100 ppm is the superposition of two components: Si(3Si)OH and Si(1Al)OH, both associated with the presence of a silicon atom connected with a single OH group. Although the fitted signal at −100 ppm is wider for the samples with lower Si/Al ratio (Fig. 4) further deconvolution of this signal would be ambiguous. The intensity change of the −100 ppm signal is not monotonic with Si/Al because the intensity decrease caused by decreasing Al amount is accompanied by change in the SiOH groups concentration (Fig. 1a).

In MCM-22 zeolites, the ^{27}Al NMR signal due to tetrahedral Al clearly consists of two components: at 55 and 48 ppm (Fig. 5). It is worth to note that the ratio between 55 and 48 ppm signals is changing—the higher the amount of Al (lower Si/Al), the more intense is the 55 ppm signal compared to the 48 ppm one. Since Al atoms may be located in two distinct pore systems proposed for this zeolite, the presence of the two sets of signals derived from tetrahedral Al is understandable [34]. Lippmaa et al. [35] showed that the chemical shifts of tetrahedral Al correlate with average Al–O–Si angles in zeolite frameworks and on this basis the average angles of 152° and 164° for the 55 and 48 ppm components were assigned. Keneddy et al. [17] then assigned the presence of the 55 ppm peak to the

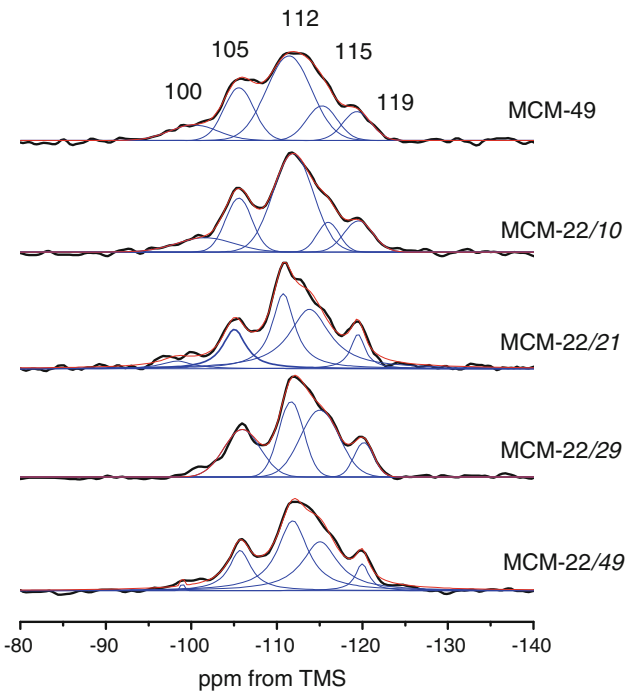

Fig. 4 ^{29}Si MAS-NMR spectra of the MWW zeolites

population of T1, T3, T4, T5, T8 sites and the 48 ppm peak to T6 and T7 sites. In this particular case the increase of the Al(Td) signal at 55 ppm can be interpreted by Al-enrichment of the T1, T3, T4, T5, T8 sites relative to the T6, T7 sites. The low number of Lewis acid centers detected by pyridine is consistent with low intensity of the 0 ppm signal due to extraframework Al.

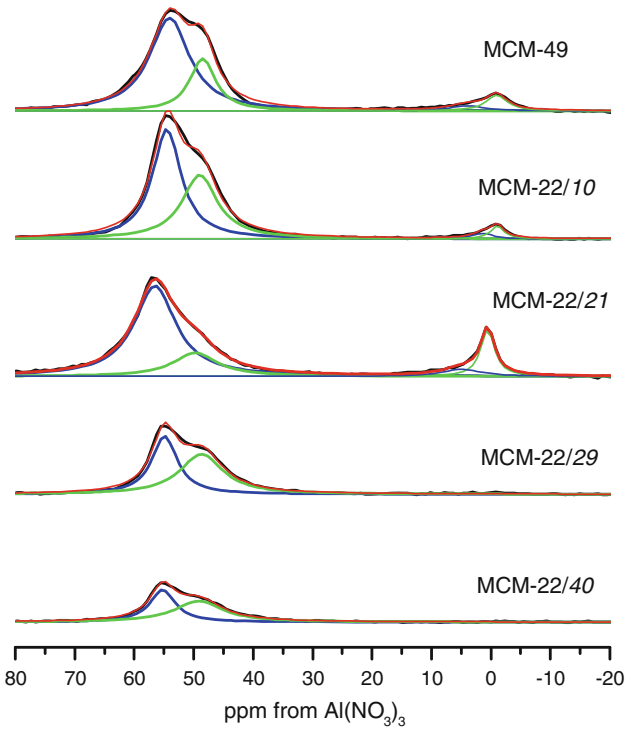

Fig. 5 ^{27}Al NMR spectra of MWW zeolites

Pyridine is unable to recognize the type of Lewis acid centers—whether they are intrinsic Lewis sites, originating from the defective aluminum atoms (placed outside the framework already during synthesis) or Lewis sites arising from dehydroxylation. The type of Lewis acid centers present was therefore determined by adsorption of CO. All MWW-type zeolite samples were activated at increasing temperatures: 100 to 700 °C, and after each activation step CO was adsorbed at −100 °C. Figure 6 shows the spectra of CO adsorption in two zeolites of similar Si/Al ratio: MCM-22/*10* and MCM-49 with higher amount of extra-framework Al. At low activation temperatures (up to 400 °C) in neither zeolite the bands due to CO bonded to Lewis acid sites are present, at the same time those centres cannot be saturated by molecular water because the bands of H–O–H bending vibrations are absent in the spectra recorded even after activation at 100 °C. At higher temperatures two bands appear: the one at 2,240 cm^{-1} is characteristic for Lewis sites resulting from dehydroxylation in all zeolites independent of their topology. The other, at 2,228 cm^{-1}, appears only as a result of dehydroxylation of a MWW structure [36]. The latter band appears first and later on both bands increase their intensities simultaneously. Careful analysis of the difference spectra suggests that the OH groups from 12- and 10-ring channels dehydroxylate first while the band characteristic of OH groups from hexagonal prisms did not decrease its intensity. In neither zeolite the bands of CO bonded to intrinsic Lewis sites (2,190 cm^{-1}) are present indicating that all the framework defects are caused by temperature treatment.

4 Strength of the Acid Sites

Acid strength of the Si–OH–Al groups can be estimated in two independent experiments: pyridine thermodesorption and CO adsorption. In the first case the determinant of the acid strength is the amount of pyridine present in zeolite after selected desorption temperature. Such experiment is in fact dependent on two factors: the intrinsic acid strength of the given OH group and diffusivity limits. In the latter case, the determinant of the acid strength of a given OH group is the value of the red-shift of its IR band, caused by its interaction with the CO molecule. The CO adsorption is a static experiment, independent of diffusion.

During CO adsorption all OH groups interact with the introduced probe molecule (Fig. 7). The red-shift of the acidic Si–OH–Al groups was the same for all MWW samples, equal to 326 cm^{-1}. On the basis of this red-shift, proton affinity (PA) can be calculated using the modified [37] Paukshtis and Yurchenko equation [38]: $PA = PA_{st} - 442.5 \log(\Delta\nu)$. The value of 1142.7 kJ/mol was determined, which is comparable to the one for LZY-82, ultra-stabilized zeolite Y ($\Delta\nu = 315$ cm^{-1}, PA = 1149.5 kJ/mol), much lower than for ZSM-5 ($\Delta\nu = 310$ cm^{-1}, PA = 1152.4 kJ/mol) or ferrierite ($\Delta\nu = 293$ cm^{-1}, PA = 1163.2 kJ/mol) indicating much higher acid strength of Si–OH–Al groups in MWW-type zeolites, irrespective of their Si/Al ratio or synthesis method. On the basis of CO adsorption it is impossible to determine the red-shift of OH groups located in hexagonal prisms (the band at 3,582 cm^{-1}). Even very careful analysis of the subtraction spectra is not revealing any additional red-shifted components suggesting that all types of Si–OH–Al groups have the same acid strength. The dependence between the half-width of the IR bands of the hydrogen-bonded OH groups ($\Delta\nu_{1/2}$) on the value of this red-shift ($\Delta\nu$) can be also used to determine heterogeneity of the acid centers. For that purpose the method of investigation of the heterogeneity of Si–OH–Al groups in zeolites taken from our previous work [39] is applied. Figure 7b shows the line being the upper limit of the dependence of $\Delta\nu(\Delta\nu_{1/2})$ for the compounds containing homogeneous OH groups (zeolite A, dealuminated Beta and NaHX among others). The point for all MWW materials from the current work is located below the line which is the evidence of homogeneity of the acid strength of the Si–OH–Al groups in all of the investigated samples.

The pyridine thermodesorption experiment points to differences of acid strength among the investigated zeolites (Table 1) the result which is in contradiction to the results of CO adsorption. The values of A_{520}/A_{250}, where A_{520} is

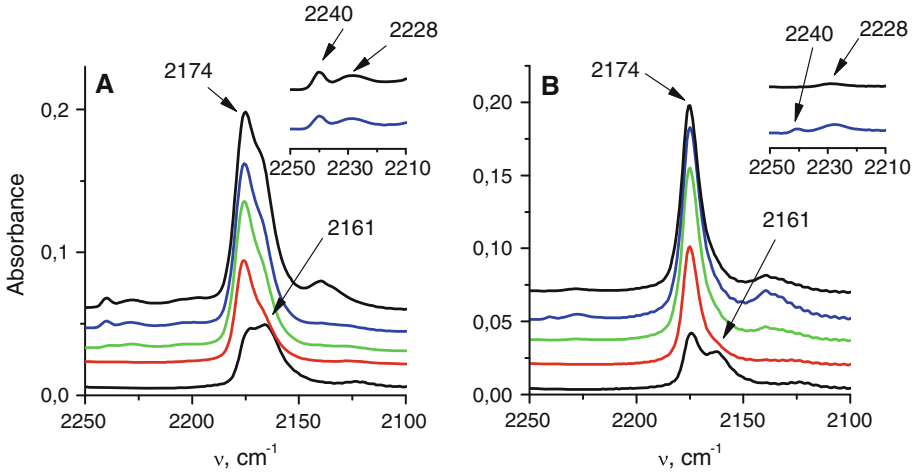

Fig. 6 Spectra of CO adsorbed on MCM-49 (**a**) and MCM-22/*10* (**b**) activated at increasing temperatures. From bottom to top 300, 400, 500, 600, and 700 °C . All spectra normalized to 10 mg pellet

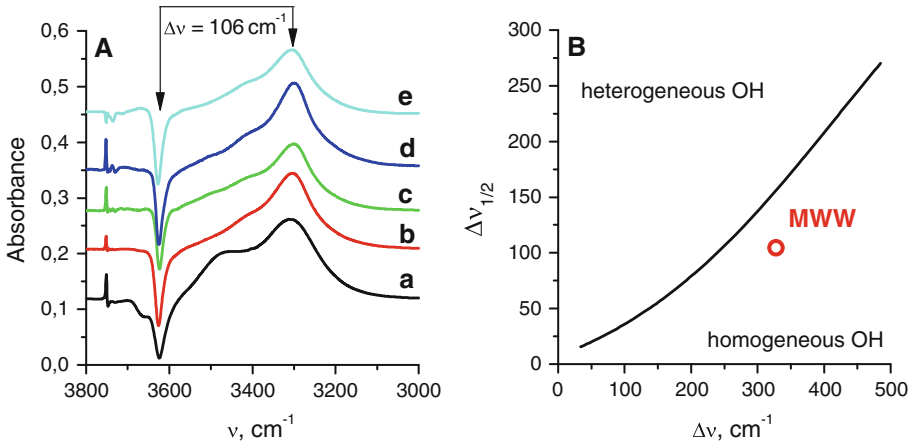

Fig. 7 **a** IR spectra of OH groups interacting with CO in MWW zeolites activated at 500 °C: MCM-49 (*a*), MCM-22/*10* (*b*), MCM-22/*21* (*c*), MCM-22/*29* (*d*) and MCM-22/*40* (*e*). Background spectra of activated samples were subtracted. **b** *line* showing the dependence of the $\Delta\nu_{1/2}$ (half-width of the red-shifted band of OH groups) on $\Delta\nu$ (the value of the red-shift caused by CO adsorption) for homogeneous OH groups (from [26]) and the point for investigated MWW zeolites

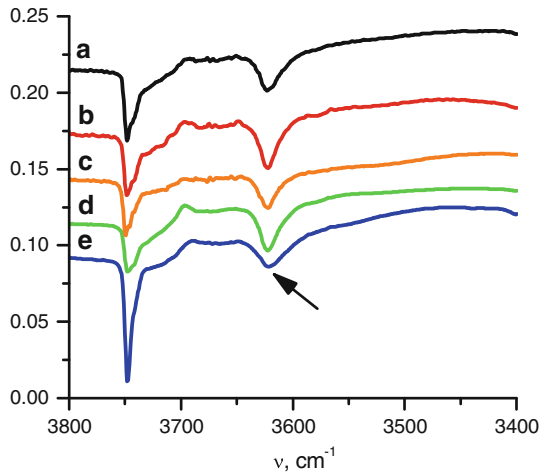

Fig. 8 IR spectra of OH groups interacting with pivalonitrile in MWW zeolites activated at 500 °C: MCM-49 (*a*), MCM-22/*10* (*b*), MCM-22/*21* (*c*), MCM-22/*29* (*d*) and MCM-22/*40* (*e*). Background spectra of activated samples were subtracted

the intensity of the pyridinium ion band at 1,545 cm^{-1} after desorption at 520 °C and A_{250} is the maximum intensity of this band (after desorption at 250 °C) is taken as the direct measure of the acid strength of OH groups in MWW zeolites. Higher values of A_{520}/A_{250} point to higher acid strength of the acidic centers. In this method of acidity measurement, the acid strength is in fact related not only to the "intrinsic" acid strength of the OH groups but also to some extent to the diffusion limitation—especially when the channel dimensions in the given zeolite structure are similar to the kinetic diameter of the probe molecule used during the test. In the case of MWW zeolites, the dimensions of 10-rings channels (4.0 × 5.5 and 4.1 × 5.1 Å) are similar to pyridine kinetic diameter (5 Å) therefore the diffusion limitation may influence the measurement of the acid strength. The values A_{520}/A_{250} are indicating the acidity order: MCM-22/*40* > MCM-49 > MCM-22/*10* > MCM-22/*21* > MCM-22/*29*. This order is following

Table 1 Physicochemical characterization of the MWW samples

Sample	BET (m^2/g)	Si/Al (XRF)	Si/Al (IR)	Al_{fram}/Al_{extraf}	C_{BAS}/C_{LAS}	A_{520}/A_{250}	External OH/u.c.
MCM-49	490	8	12	10.4	9.1	0.53	0.22
MCM-22/10	542	14	10	21.2	12.1	0.43	0.36
MCM-22/21	418	33	21	2.1	13.7	0.36	0.22
MCM-22/29	481	31	29	–[a]	13.1	0.25	0.28
MCM-22/40	329	42	40	–[a]	12.6	0.46	0.28

[a] Intensity of the 0 ppm band is below detection limit

the Si/Al ratio increase with the exception of the MCM-22/*40* sample. In the latter case however, it can be supposed that crystallites may form small aggregates, effectively elongating the diffusion path. It is worth mentioning that even for the MCM-49 sample, which has the highest aluminum content, all acidic Si–OH–Al may be considered as isolated, therefore all of them should display uniform and high acid strength as it was proven by the experiment of CO adsorption. The apparent different acid strengths for the series of MWW-type zeolites is most probably due to diffusion limitations, which is most likely caused by pyridine readsorption on the neighboring acid centers as it migrates along the channel. Channel exits are located on the side walls of MWW crystals, which means that a desorbing molecule has to diffuse along the whole crystal, thus the probability that it will encounter and re-adsorb on the subsequent acid centers depends on the concentration of the acid sites and should diminish with the increasing Si/Al. Such trend was also observed with other measurement methods [40, 41].

5 Pivalonitrile Sorption: Studies of the Accessibility of Si–OH–Al Groups

One of the most interesting features of MWW zeolites is the presence of acidic OH groups on the external surface of the crystals. This imparts a particular type of catalytic activity, which has been successful for application in the industry and MCM-22 is commercially used as the catalyst for ethylbenzene synthesis and cumene [42]. To study accessibility of the OH groups located inside these external 'cups' pivalonitrile adsorption was performed. Application of pivalonitrile as a probe molecule for testing external acidity of zeolites was proven useful by the group of Busca and co-workers [43]. The presence of *tert*-butyl group prevents entrance into the 10-ring openings and therefore restricting any interaction to the external surface of the MWW-type zeolites. Pivalonitrile is interacting only with fraction of the OH groups—those located at the external 'cups' or very nearly the pore entrances while is not interacting with the OH groups located in the hexagonal prisms in between the supercages (the difference band is not containing the submaximum at 3,582 cm^{-1}). First, pivalonitrile was adsorbed at RT and afterwards its excess desorbed for 5 min at high vacuum ($\sim 10^{-4}$ mBa). Then, from the intensity of the 3,621 cm^{-1} band consumed by pivalonitrile (Fig. 8) and its integrated absorption coefficient calculated by Ayrault et al. [44] and equal 2.5 cm/μmol, the concentration of the external acidic OH groups was calculated. As can be seen from the data presented in Table 1, the number of external OH groups is basically independent of the Si/Al ratio, sample origin and the synthesis method. This would suggest that, at least for the series investigated in the current work, any reaction occurring exclusively at the external zeolite surface should occur with very similar selectivity and yield.

6 ETBE Synthesis

As the test reaction the synthesis of ETBE from the equimolar mixture of ethanol and isobutene was chosen.

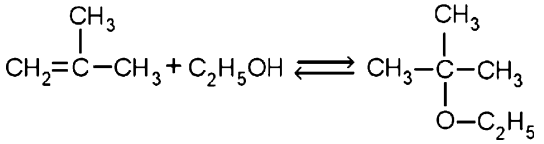

Because of the presence of the *tert*-butyl group even if such ether could have been formed inside the MWW supercage (both ethanol and isobutene can easily penetrate MWW micropores), its diffusion out of the zeolite channel system through the 10-ring openings would be impossible. Any ETBE molecule detected by the chromatography must have been therefore formed in the 'cups' at the external surfaces of the crystals. Reaction was performed at 80 °C because of too low yield at 60 °C (ca. 3%) while at 100 °C ETBE decomposition would occur. Two products of ethanol and isobutene reaction were present: ETBE and *tert*-butyl alcohol (product of the side reaction $C_4H_8 + H_2O = (CH_3)_3COH$, with the remaining water from ethanol); the latter with yield below 0.6% and formed also on the external zeolite surface. For the catalytic reaction only three samples, with different Si/Al ratio and the method of

Table 2 Catalytic performance of selected samples in ETBE synthesis from ethanol and isobutene at equimolar ratio (average from five measurements)

Sample	EtOH conversion to ETBE (%)	Yield of ETBE (%)	Yield of TBA (%)
MCM-49	10.0 ± 0.89	3.91 ± 0.11	0.56 ± 0.015
MCM-22/21	9.51 ± 1.03	3.91 ± 0.13	0.57 ± 0.063
MCM-22/29	9.79 ± 1.46	3.52 ± 0.42	0.56 ± 0.047

synthesis were chosen. In all cases ethanol conversion to ETBE was virtually constant, as was the yield (Table 2).

As it was shown that ETBE synthesis was conducted exclusively at the external zeolite surface the fact that ether yield was constant corroborates the hypothesis that the concentration of the active centers at the external 'cups' was constant for all samples.

7 Conclusions

A series of MWW-type zeolites: MCM-22 samples with increasing Si/Al ratio and an MCM-49 zeolite were investigated with respect to their acidic properties. The total concentration of Brønsted acid centers derived from the pyridine adsorption experiment followed by IR spectroscopy matched very well the Si/Al ratio determined by the XRF.

Two types of the framework as well as extraframework aluminum was confirmed by ^{27}Al MAS-NMR. The ratio between the 48 and the 55 ppm signals changed with the Si/Al ratio. This can be interpreted by Al-enrichment of the T1, T3, T4, T5, T8 sites compared to the T6, T7 sites with increasing Al content.

OH groups in MWW zeolites were found to be homogeneous, with low PA value (high acid strength) equal to 1142.7 kJ/mol, which is comparable to the one for steamed HY zeolite and lower than in ZSM-5. Diffusivity was found to be very important determinant of the activity (in the terms of the apparent acid strength).

Concentration of Brønsted acid centers located on the external crystal surface was invariant for the entire series. This fact was further confirmed in the test reaction of ETBE synthesis from ethanol and isobutene which could be occur only at the external crystal surfaces and not inside due to sterical restrictions. Ethanol conversion to ETBE as well as the ether yield was constant.

Acknowledgments The research was carried out with the equipment purchased thanks to the financial support of the European Regional Development Fund in the framework of the Polish Innovation Economy Operational Program (Contract no. POIG.02.01.00-12-023/08). IR measurements were made in the frames of the grant from the Ministry of Science and Higher Education, Warsaw (Project no. NN204 1987 33).

References

1. Auroux A (2002) Top Catal 19:205
2. Čejka J, Wichterlová B (2002) Catal Rev 44:375
3. Corma A (1995) Chem Rev 95:559
4. Gil B, Zones SI, Hwang S-J, Bejblová M, Čejka J (2008) J Phys Chem C 112:2997
5. Lercher JA, Gründling C, Eder-Mirth G (1996) Catal Today 27:353
6. Wichterlová B, Čejka J (1992) Catal Lett 16:421
7. Weber RW, Möller KP, O'Connor CT (2000) Micropor Mesopor Mater 35:533
8. Leonowicz ME, Lawton JA, Lawton SL, Rubin MK (1994) Science 264:1910
9. Camblor MA, Corell C, Corma A, Diaz-Cabanas M-J, Nicolopoulos S, Gonzalez-Calbet JM, Vallet-Regi M (1996) Chem Mater 8:2415
10. Camblor MA, Corma A, Diaz-Cabanas M-J, Baerlocher Ch (1998) J Phys Chem B 102:44
11. Zones SI, Hwang SJ, Davis ME (2001) Chem Eur J 7:1990
12. Puppe L, Weisser J (1984) US Patent 4,439,409
13. Belussi G, Perego G, Clerici MG, Giusti A (1988) European Patent Application, EPA 293032
14. Roth WJ (2007) Stud Surf Sci Catal 168:221
15. Kennedy GJ, Lawton SL, Fung AS, Rubin MK, Steuernagel S (1999) Catal Today 49:385
16. Aiello R, Crea F, Testa F, Demortier G, Lentz P, Wiame M, Nagy JB (2000) Micorpor Mesopor Mater 35–36:585
17. Kennedy GJ, Lawton SL, Rubin MK (1994) J Am Chem Soc 116:11000
18. Dědeček J, Čejka J, Oberlinger M, Ernst S (2002) Stud Surf Sci Catal 142 A:23
19. Van Miltenburg A, Pawlesa J, Bouzga AM, Žilková N, Čejka J, Stöcker M (2009) Top Catal 52:1190
20. Degnan TF Jr, Morris Smith C, Venkat CR (2001) Appl Catal A 221:283
21. Park S-H, Rhee H-K (2000) Catal Today 63:267
22. Čejka J, Krejci A, Zilkova N, Kotrla J, Ernst S, Weber A (2002) Micropor Mesopor Mater 53:121
23. Delitala C, Alba MD, Becerro AI, Delpiano D, Meloni D, Musu E, Ferino I (2009) Micropor Mesopor Mater 118:1
24. Pawlesa J, Zukal A, Čejka J (2007) Adsorption 13:257
25. Mokrzycki Ł, Sulikowski B, Olejniczak Z (2009) Catal Lett 127:296
26. Rhodes CJ (2008) Prog React Kinet Mech 33:1
27. Katada N, Niwa M (2004) Catal Surv Asia 8:161
28. Datka J, Sulikowski B, Gil B (1996) J Phys Chem 100:11242
29. Engelhardt G, Lohse U, Patzelova V, Mägi M, Lippmaa H (1983) Zeolites 3:233
30. Onida B, Geobaldo F, Testa F, Aiello R, Garrone E (2002) J Phys Chem B 106:1684
31. Thibault-Starzyk F, Gil B, Aiello S, Chevreau T, Gilson J-P (2004) Micropor Mesopor Mater 67:107
32. Datka J, Gil B, Kubacka A (1996) Zeolites 17:428
33. Makarova MA, Karim K, Dwyer J (1995) Micropor Mater 4:243
34. Kolodziejski W, Zicovich-Wilson C, Corell C, Perez-Pariente J, Corma A (1995) J Phys Chem 99:7002

35. Lippmaa E, Samoson A, Mägi M (1986) J Am Chem Soc 108:1730
36. Góra-Marek K, Datka J (2005) Stud Surf Sci Catal 158A:83
37. Datka J, Broclawik E, Gil B (1994) J Phys Chem 98:5622
38. Paukshtis EA, Yurchenko EN (1983) Usp Khim 52:426
39. Datka J, Gil B (2001) Catal Today 70:131
40. Meloni D, Laforge S, Martin D, Guisnet M, Rombi E, Solinas V (2001) Appl Catal A 215:55
41. Okumura K, Hashimoto M, Mimura T, Niwa M (2002) J Catal 206:23
42. Corma A, Martínez-Soria V, Schnoeveld E (2000) J Catal 192:16
43. Bevilacqua M, Meloni D, Sini F, Monaci R, Montanari T, Busca G (2008) J Phys Chem C 112:9023
44. Ayrault P, Datka J, Laforge S, Martin D, Guisnet M (2004) J Phys Chem B 108:13755